Water Soluble Polymers. 74. pH Responsive Microdomains in Labeled *n*-Octylamide-Substituted Poly(sodium maleate-*alt*-ethyl vinyl ethers): Synthesis, Steady-State Fluorescence, and Nonradiative Energy Transfer Studies

Yuxin Hu, Geoffrey L. Smith, Michael F. Richardson, and Charles L. McCormick*

Department of Polymer Science, University of Southern Mississippi, Southern Station Box 10076, Hattiesburg, Mississippi 39406

Received September 10, 1996; Revised Manuscript Received February 19, 1997[⊗]

ABSTRACT: *n*-Octylamide-substituted copoly(sodium maleate-*alt*-ethyl vinyl ethers) [poly(SM−EVEs)] have been synthesized and fluorescently labeled with naphthyl and/or dansyl chromophores attached to the polymer backbone with either a long (C8) or short (C2) carbon spacer. The chromophores serve as monitors of the local environmental character of these amphiphilic macromolecules as they undergo the "polysoap-to-polyelectrolyte" transition. Intramolecular (closed) associations tend to predominate over a wide range of environmental conditions in aqueous media. The extent and reversibility of these interactions have been investigated by conducting viscometric measurements, light scattering, nonradiative energy transfer (NRET) quantum efficiency, and fluorescence quenching studies as a function of the solution pH. The results obtained for the 30% *n*-octylamide-modified poly(SM−EVE) in aqueous media have been contrasted with results obtained for 30% *n*-octylamide-modified poly(SM−EVE) in 6 M urea solution and unmodified poly(SM−EVE) in aqueous media to provide meaningful information concerning the effect of hydrophobic modification and pH responsiveness. The octylamide-modified polymer in aqueous media at low pH collapses into a compact aggregate due to the loss of polyelectrolyte character and an increase in hydrogen bonding. At moderate pH values, the modified polymer coil becomes slightly more expanded, as indicated by fluorescence and reduced viscosity measurements. At pH values between 7.0 and 8.0, the most expanded conformation is observed as determined by hydrodynamic size and nonradiative energy transfer (NRET) quantum efficiency measurements. NRET studies of both singly- and doubly-labeled, hydrophobically modified polymer solutions and fluorescence quenching in aqueous media are consistent with a globule-to-extended chain transition with increasing pH. At low pH, however, multichain complexes appear to form, even in dilute solution. At higher concentrations, above *C**, multichain interactions are observed, consistent with associative thickening observed by viscometry. The onset values of *C** in these systems as sensed by NRET are nearly one order of magnitude lower than those observed by viscometry. Also, the labels with long spacers are more sensitive than those with short spacers in detecting organized microdomains.

Introduction

Amphiphilic polymers capable of forming microphase-separated domains in aqueous media have widespread technological applications in water treatment, enhanced oil recovery, controlled-release, and formulation of water-borne coatings and personal care products.[1−3] The extent and reversibility of domain association depend on a number of intrinsic and extrinsic factors including microstructure, charge distribution, molecular weight, temperature, electrolyte concentration, and pH.[4−9] Two modes of interaction are generally envisioned arising from closed (intramolecular) and open (intermolecular) association in aqueous media. In the former, micelle-like, uni- or multimolecular aggregates form, while in the latter, network-like structures are common. Although the macroscopic solution properties of these two extremes in association type are quite diverse, e.g. surface activity vs viscosification, the "hydrophobic effect" has been proposed as the major contributor to structural ordering.

A number of experimental techniques[9−16] have been utilized to study the nature of microphase-separated domains in aqueous media, including viscometry,[9−10] light scattering,[11−14] and NMR.[15,16] Photophysical methods[17−21] have been especially useful in studying hydrophobic domain organization and dynamics for both nonionic[22−25] and polyelectrolyte systems.[11,14,21,26−30] Fluorescence quenching studies have been designed, not only to establish aggregation behavior[21,25,26,28,31−34] but also to estimate the size of domains formed by hydrophobic association in aqueous media.[35−39] In addition, nonradiative energy transfer studies,[17−20,22,31,40−45] have provided convincing evidence regarding the morphology of phase-separated microdomains.

In pursuit of our overall goal of tailoring responsive polymers,[9,10,14,46−50] we continue to examine the organization and dynamics of phase-separated microdomains in aqueous media. On the basis of the seminal work of Strauss and co-workers,[51−55] we have developed synthetic strategies that can produce a continuum of properties ranging from "polysoap" to "associative thickening". We concentrate in this report on the pH responsiveness of specifically labeled, *n*-octylamide-substituted poly(sodium maleate-*alt*-ethyl vinyl ethers), which form predominantly closed (intramolecular) associations in dilute aqueous solutions.

As will be evident from the discussion to follow, the nature of the fluorescence labels, the polymer microstructure arising from the prescribed synthesis, and specified environmental conditions allow us to demonstrate pH-dependent associations including multimolecular aggregation. Elucidation of this mechanism clarifies a number of issues and illustrates that the "unimolecular micelle" conceptual model for hydropho-

[⊗] Abstract published in *Advance ACS Abstracts,* May 1, 1997.

S0024-9297(96)01350-2 CCC: $14.00

Scheme 1. Synthetic Pathway for Preparation of Hydrophobically Modified Copoly(sodium maleate-*alt*-ethyl vinyl ethers) with Fluorescent Labels

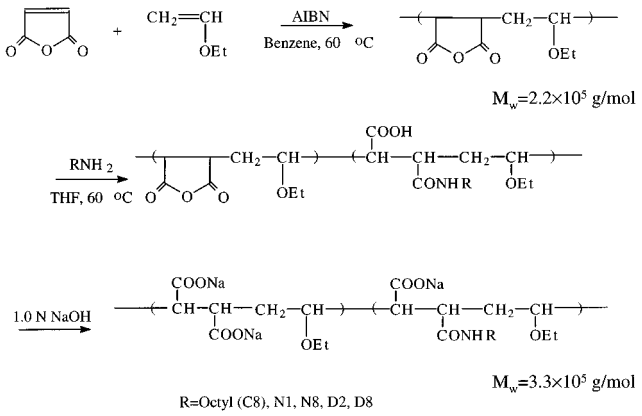

bically-modified polymers is valid only under certain conditions. We establish the pH-responsive behavior of these specifically labeled systems in two reports. In this manuscript we utilize steady-state fluorescence, nonradiative energy transfer (NRET), and quasielastic light scattering methods. In a subsequent study,[56] we describe in detail transient fluorescence and time-resolved anisotropy results. NRET of naphthyl to pyrenyl labels was used previously in our lab,[46,47] to study intramolecular and intermolecular associations of 30% *n*-octylamide-modified copoly(SM−EVEs). However, the pyrenyl labels exhibit a tendency to "organize" rather than "report" domain hydrophobicity and the necessity to correct for significant pyrenyl emission limited the extent of quantitative interpretation.

Experimental Section

Materials. All commercial chemicals and solvents were purchased from Aldrich Chemical Co. unless otherwise designated. Benzene and tetrahydrofuran (THF) were dried for 24 h over calcium hydride and distilled under nitrogen. Maleic anhydride was recrystallized twice from chloroform. Ethyl vinyl ether (bp 32−33.5 °C) was distilled twice at atmospheric pressure before use. 2,2′-Azobis(2-methylpropionitrile) (AIBN) was recrystallized from methanol. Other materials were used as received. The water used was deionized and was found to possess a conductance $<10^{-7}$ Ω/cm.

Dansyl-2-aminocaprylic acid (**1**) and succinic acid *N*-(1-naphthylmethyl)monoamide (**2**) were chosen as model compounds (see Figure 1). The former was purchased from Sigma and was recrystallized from methanol. A procedure reported previously by our lab was employed to synthesize **2**.[46] The NRET donors used for labeling the copolymer backbone were 1-naphthylmethylamine (N1) and 7-(1-naphthylmethoxy)heptylamine (N8). N1 was purchased from Aldrich, and N8 was synthesized using the methods of McCormick and Chang.[9] The NRET acceptors, 2-dansylethylamine (D2) and 8-dansyloctylamine (D8), were both synthesized as described by Shea et al.[57] The structures of these chromophores, N1, N8, D2, and D8, are also shown in Scheme 1.

The synthesis of the labeled copoly(SM−EVE) has been described previously.[46] Structures and subsequent modifications are depicted in Chart 1. In our previous work, the M_w of poly(maleic anhydride-*alt*-ethyl vinyl ether) [poly(MA−EVE)] prepared under these conditions was found to be 2.2 × 10^5 in THF and the M_w of 30 mol % *n*-octyl hydrophobically modified poly(SM−EVE) was found to be 3.5 × 10^5 in aqueous solution, as determined by classical light scattering methods. Copolymer compositions were determined from ^{1}H, gated-decoupled ^{13}C NMR and UV absorption data and are shown in Table 1.

Instrumentation. Viscosity measurements were conducted with a Contraves LS-30 low-shear rheometer at a constant shear rate of 5.96 s^{-1} at 25 °C. A Bruker AC-200 NMR spectrometer was used to obtain ^{1}H, ^{13}C and gated-decoupled ^{13}C NMR spectra. NMR spectra were determined in either acetone-d_6 with 1% (v/v) TMS as an internal standard for the unhydrolyzed polymer or in deuterium oxide with 1% (w/w) DSS as an internal standard for hydrolyzed polymers. All UV−vis spectra were recorded with a Hewlett-Packard 8452A diode array spectrophotometer. Excitation and emission spectra were measured at 25 °C with an Edinburgh FS900CDT T-Geometry fluorometer.

Chart 1. Model Compounds 1 and 2 and Fluorescent Labels N1, N8, D2, and D8

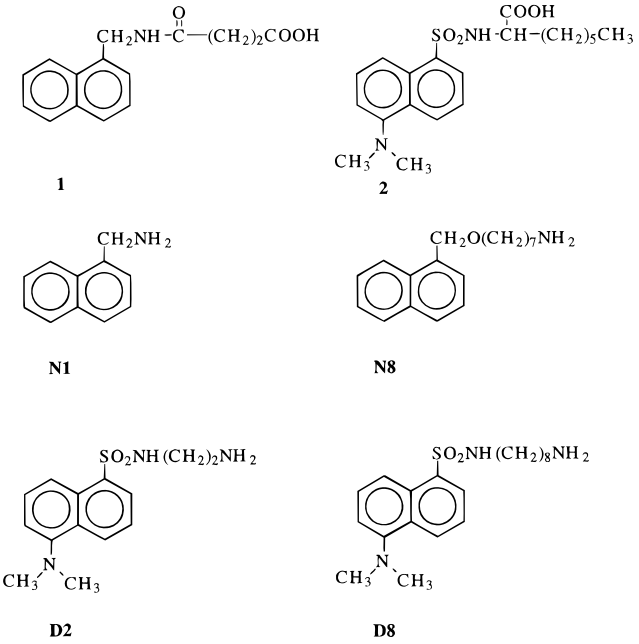

Table 1. Composition of *n*-Octylamide-Mofied and Unmodified Copoly(Sodium Maleate-*alt*-Ethyl Vinyl Ethers)

polymer	C8 content (mol %)[a]	naphthalene content (mol %)[b]	dansyl content (mol %)[b]
C8	30		-
C8-N1	31	1.0	-
C8-D2	30		1.0
C8-N1-D2	30	1.2	1.0
C8-N8	32	1.1	-
C8-D8	30		1.0
C8-N8-D8	30	1.1	1.0
C0			
C0-N1		1.1	
C0-D2			1.0
C0-N1-N2		1.0	1.0
C0-N8		1.1	
C0-D8			1.0
C0-N8-D8		1.1	1.0

[a] From ^{1}H and gate-decoupled ^{13}C NMR (D_2O) data. [b] From UV absorption data.

Light Scattering Measurements. Classical and dynamic light scattering measurements were made with a Brookhaven BI-DS low-angle laser light scattering spectrometer at 25 °C. All classical measurements were performed as previously reported.[14] Values of the refractive index increment, d*n*/d*c*, for copoly(MA−EVEs) in THF ranging 1.5−0.3 g/L and 30% octylamide-modified copoly(SM−EVEs) in water ranging 2.0−0.3 g/L were determined using a Chromatix KMX-16 laser differential refractometer at 25 °C. The values of d*n*/d*c* are 0.1161 for copoly(MA−EVEs) and 0.1354 for 30% octylamide-modified copoly(SM−EVEs). Zimm plots of the copolymers were obtained between 45 and 110 °C and the copolymer concentrations mentioned above. Dynamic measurements were performed using Brookhaven Instruments model 2030AT digital correlator, and a 633 nm laser was used as the light

Table 2. Composition of Copolymer Solutions Prepared for Fluorescence Energy Transfer Measurements

30% *n*-Octylamide-Substituted Short Spacer Labels

solution	[C8] (g/L)	[C8-N1] (g/L)	[C8-D2] (g/L)	[C8-N1-D2] (g/L)	[naphthyl] (mol/L) × 10^{-6}	[dansyl] (mol/L) × 10^{-6}
C8/C8-N1	0.25	0.25			9.6	-
C8/C8-D2	0.25		0.25		-	9.6
C8-N1/C8-D2		0.25	0.25		9.6	9.6
C8/C8-N1-D2	0.25			0.25	11.4	9.5

30% *n*-Octylamide-Substituted Long Spacer Labels

solution	[C8] (g/L)	[C8-N8] (g/L)	[C8-D8] (g/L)	[C8-N8-D8] (g/L)	[naphthyl] (mol/L) × 10^{-6}	[dansyl] (mol/L) × 10^{-6}
C8/C8-N8	0.25	0.25			10.5	
C8/C8-D8	0.25		0.25			9.5
C8-N8/C8-D8		0.25	0.25		10.5	9.5
C8/C8-N8-D8	0.25			0.25	10.4	9.4

Unsubstituted Short Spacer Labels

solution	[C0] (g/L)	[C0-N8] (g/L)	[C0-D8] (g/L)	[C0-N8-D8] (g/L)	[naphthyl] (mol/L) × 10^{-6}	[dansyl] (mol/L) × 10^{-6}
C0/C0-N1	0.25	0.25			11.8	
C0/C0-D2	0.25		0.25			10.7
C0-N1/C0-D2		0.25	0.25		11.8	10.7
C0/C0-N1-D2	0.25			0.25	10.6	10.6

Unsubstituted Long Spacer Labels

solution	[C0] (g/L)	[C0-N8] (g/L)	[C0-D8] (g/L)	[C0-N8-D8] (g/L)	[naphthyl] (mol/L) × 10^{-6}	[dansyl] (mol/L) × 10^{-6}
C0/C0-N8	0.25	0.25			11.7	
C0/C0-D8	0.25		0.25			10.6
C0-N8/C0-D8		0.25	0.25		11.7	10.6
C0/C0-N8-D8	0.25			0.25	11.6	10.5

source. The intensity correlation function was recorded and fit using the CONTIN analysis algorithm provided by Brookhaven Instruments. All dynamic measurements were made at an angle of 90°.

Solution Preparation and Measurements. Aqueous solutions of poly(SM−EVE) modified with *n*-octylamide groups were used for viscosity studies. Aqueous polymer stock solutions for each modified polymer were prepared and allowed to stand for 24 h before dilution in order to reach equilibrium in micelle-forming. All copolymer solutions were diluted to 0.50 g/L for dynamic light scattering and fluorescence measurements. On the basis of the viscosity results, this concentration was chosen since it is well below C^* for the polymer, thus allowing the opportunity to monitor conformational changes of individual polymer chains. The solution compositions are shown in Table 2. HCl and NaOH (0.1 N) were used to adjust the pH in preparing the aqueous solutions for measurements. For UV−vis absorption measurements, water was used as the blank. All solutions were degassed by vigorous bubbling with nitrogen for 15 min before fluorescence measurements were performed. All emission and excitation spectra were corrected. For emission measurements, slit widths were set at 2.0 nm at both excitation and emission positions, and scan rates were set at 1.0 nm/s.

Fluorescence Quantum Yield. Prior to quantum yield determination, the absorbance of the dansyl labels at 330 nm and naphthyl labels at 282 nm for a polymer concentration of 0.50 g/L was determined. This then allowed the calculation of the fluorescence quantum yield using the equation

$$\Phi_x = \Phi_{st} \frac{A_{st}}{A_x} \frac{I_x}{I_{st}} \frac{n_x^2}{n_{st}^2} \tag{1}$$

where Φ is the quantum yield, A is the absorbance at the excitation wavelength, I is the integral area of the corrected emission spectrum, and n is the reflective index at the excitation wavelength. The subscript x refers to the utilized chromophore and the subscript st refers to the standard compound.

Nonradiative Energy Transfer. For NRET measurements, an Acton cutoff WG-305 optical filter was used at the excitation wavelength (282 nm) to prevent scattering of the excitation beam from the samples. The dansyl chromophores were excited at 330 nm to observe the dansyl emission spectra. Quantum yields (Φ) of the naphthyl chromophores were calculated by integrating the areas of the corrected emission spectra in reference to 2-aminopyridine in 0.10 N H_2SO_4 as the standard ($\Phi = 0.60$ at 282 nm excitation).[58] Quantum yields (Φ) of the dansyl labels excited at 330 nm were calculated by integrating the areas of corrected emission spectra in reference to quinine bisulfate in 1.0 N H_2SO_4 as the standard ($\Phi = 0.55$ at 330 nm excitation).[59] Beer's law corrections were applied for optical density changes at the excitation wavelength. Corrections were also made for refractive index differences.

The Förster distance, r_o, has been previously determined to be 23.45 Å for the naphthalene/dansyl donor/acceptor pair,[60] and the NRET quantum efficiency, χ, has been calculated using the method described by Guillet.[43] In this case, the modified Guillet method[46] is used for calculating NRET quantum efficiency, χ, due to the minor absorbance of the dansyl chromophore when 282 nm is used as the excitation wavelength. The modified Guillet equation is given below:

$$\frac{\chi}{1-\chi} = \frac{\Phi_D^0 (I_A - I_A^0)}{\Phi_D^0 I_D} \tag{2}$$

in which $\Phi_D{}^0$ is the fluorescence emission quantum yield of the donor in the absence of acceptor-labeled polymer excited at 282 nm and $\Phi_A{}^0$ is the fluorescence emission quantum yield of the acceptor on the acceptor-labeled polymer. I_A and I_D are the integrated emission intensities of donor and acceptor, respectively, in the presence of both donor- and acceptor-labeled polymer, and $I_A{}^0$ is the integrated emission intensity of the acceptor in the absence of donor-labeled polymer.

Fluorescence Quenching. In order to determine the number of hydrophobic moieties on a polymer chain which constitute a microdomain, steady-state fluorescence quenching methods were utilized. All quenching studies were performed utilizing naphthalene as the donor and 9-methylanthracene (9-MA) as the quencher. Both naphthalene probe and labels were utilized to assess the effect of donor localization within

the hydrophobic microdomain. For the system containing naphthyl label, a 30% octylamide-modified copoly(SM−EVE) polymer further modified with either the long- or short-spaced naphthyl label was synthesized. Solutions of the labeled polymer were made such that the polymer concentration was 0.50 g/L and the naphthyl chromophore concentration was 20 μM. Similarly, solutions of the probe-containing system were prepared by adding sufficient naphthalene to a 0.50 g/L nonlabeled solution of modified copoly(SM−EVE) to give a chromophore concentration of 20 μM. 9-Methylanthracene (9-MA) was used as the quencher at different concentrations ranging between 0.25 and 1.5 mM. 9-MA (Aldrich) was recrystallized twice from ethanol. It was brought to the desired concentration by adding 0.10−1.00 mL of a 2.0×10^{-3} M methanol stock solution to 200.0 mL of the naphthyl donor-containing polymer solutions described above. The quenching systems were excited at 282 nm, and their emission was measured between 300 and 520 nm. All quenching solutions were allowed to stand for 2 days and were degassed using sequential vacuum−N_2 flushing cycles for 2 h before fluorescence measurements were performed.

For steady-state fluorescence quenching (SSFQ), the emission spectrum of a naphthyl chromophore was measured in the presence of increasing amounts of the luminescence quencher, 9-MA. The naphthyl chromophore intensities in the absence (I_0) and presence (I) of quencher obey the equation[36−38]

$$\ln(I_0/I) = [Q]/[M] \tag{3}$$

The slope of the plot of $\ln(I_0/I)$ versus [Q] yields the micelle concentration [M], and in turn the micelle aggregation number (NSSFQ) is given by

$$N_{SSFQ} = (C - \text{cmc})/[M] \tag{4}$$

where C is the total concentration of octylamide groups in solution and, as is customary for polymers, the cmc for the polymer with intramolecular aggregation is taken as zero.

Fluorescence decay measurements were also performed on the naphthyl/9-MA quenching system at a selected high pH value (∼9) and a low pH value (∼2−3) to confirm the applicability of steady-state quenching methods in this study. The decay of the naphthyl chromophore and 9-MA were monitored at 325 and 415 nm, respectively, when excited at 282 nm.

Results and Discussion

Copolymer Structure. In order to achieve our desired objective of elucidating the pH-responsive nature of microdomains of polymeric surfactants, we have tailored and labeled octylamide-substituted poly(sodium maleate-*alt*-ethyl vinyl ethers), poly(SM−EVEs). Our synthetic strategy was to target polymers with pH-responsive carboxylic acid moieties and moderate amounts of shorter alkyl side chain groups. Strauss and co-workers[54] in early, eloquent studies demonstrated a transition from hypercoils to extended coils (polysoap-to-polyelectrolyte transition) with increased ionization of hydrolyzed terpolymers of the alkyl-substituted vinyl ethers (butyl, pentyl, hexyl, octyl), ethyl vinyl ether, and maleic anhydride. Strauss[37,51−55] and Zana[39,62] have also shown that modification by large hydrophobes (decyl, dodecyl) on the same systems resulted in compact hypercoils in which the core structure could not be disrupted by ionization, even at high pH.

We followed a procedure previously reported by our group[9,46,63] (Scheme 1) to prepare both C8 (octyl)-modified and unmodified C0 (control) polymers with dansyl and/or naphthyl labels. First, poly(maleic anhydride-*alt*-ethyl vinyl ether) of molecular weight 2.2×10^5 was synthesized in THF; 30 mol % *n*-octylamide derivatives were produced under homogeneous solution conditions by amine addition to the parent polymer. Water solubility was then achieved by hydrolysis of the residual anhydride groups with aqueous NaOH. The weight average molecular weight of the resulting polymer in aqueous solution was determined to be 3.5×10^5 by classical light scattering methods. The labeled polymers were synthesized by introducing ∼1.0 mol % (relative to the anhydride units) of the labeled amines shown in Chart 1 along with the octylamine in the second step of the synthetic procedure.

The dansyl-labeled systems were prepared with one of two spacer lengths, a short spacer (D2) from 2-dansylethylamine or a long spacer (D8) from 8-dansyloctylamine. The former is more tightly coupled to the molecular backbone than the latter. These labels are reporters of the microenvironment alone or as acceptor molecules in nonradiative energy transfer (NRET) in conjunction with the short (N1) or long (N8) spacers of the donors 1-naphthylmethylamine or 7-(1-naphthylmethoxy)heptylamine, respectively.

Singly-labeled (either dansyl or naphthyl, both long and short spacers) and doubly-labeled (dansyl and naphthyl, long and short spacers) polymers were prepared. Compositions are shown in Table 1 for all copolymers including the unmodified controls, C0, with and without labels and the hydrophobically modified materials, C8, with and without labels.

Dilute Solution Behavior. Scheme 2 presents the generally-accepted conceptual model for conformational response of hydrophobically modified polymer chains in dilute solution expected for the singly- and doubly-labeled polymers. The inset plot of reduced viscosity vs pH previously reported by our group[9] for the *n*-octyl-modified poly(SM−EVEs), shows the classic polysoap-to-polyelectrolyte transition originally described by Strauss.[54] For noninteracting polymer chains in this concentration range, we would expect coil expansion as ionization along the backbone increases and disruption of the hydrophobic microdomains occurs. All labels should encounter a more hydrophilic environment, differing only by the extent of spacer link decoupling from the backbone with increasing charge−charge repulsion. Nonradiative energy transfer would be minimal in dilute solution for mixtures of singly-labeled naphthyl and singly-labeled dansyl chains since encounters of these chains are statistically unlikely. On the other hand, NRET should be apparent for the doubly-labeled chains (both dansyl and naphthyl on the same chain), but decreasing as the unimolecular coils undergo the globule-to-extended coil transition. The control polymers should act as normal polyelectrolytes rather than polysoaps since hydrophobic domains are not present. Transition to multimolecular association would be expected to occur only above the critical overlap concentration, C^*. This concentration should increase with an increase in pH.

Steady State Fluorescence Studies. In order to carry out fluorescence studies on copoly(SM−EVEs), several series of solutions were prepared with singly- or doubly-labeled polymers, with (C8) and without (C0) 30% *n*-octylamide substitution. Short or long spacers to naphthyl (N1 or N8) and to acceptor (D2 or D8) are designated. Our experiments involved mixing dilute concentrations (0.25 g/L) of the respective polymers to maintain a constant concentration. Table 2 lists polymer concentration and molar concentrations of the dansyl and naphthyl labels in each solution.

Scheme 2. Conceptual Model Illustrating pH-Induced "Polysoap-to-Polyelectrolyte" Conformational Change for Hydrophobically Modified Copolymers with Fluorescent Labels at (a) Low and (b) High Copolymer Concentrations[a]

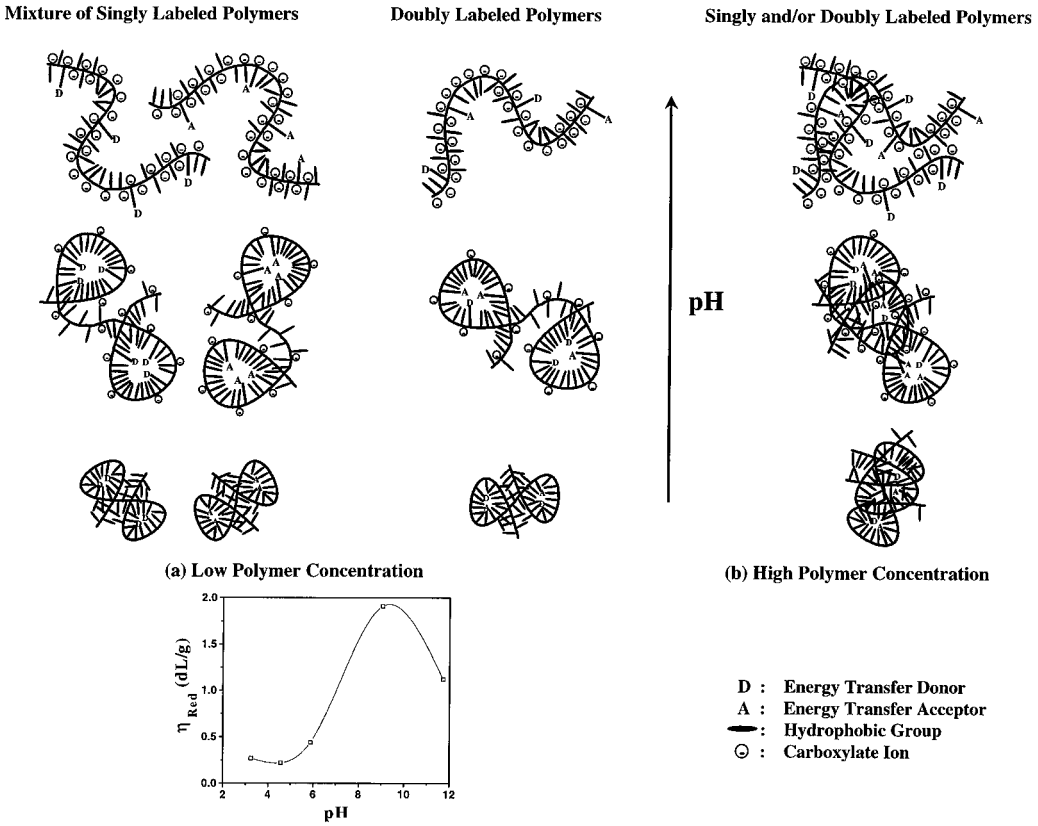

[a] Inset shows reduced viscosity as a function of pH value for a 30% *n*-octylamide-substituted copoly(SM−EVE) at a shear rate of 1.28 s^{-1}.[9]

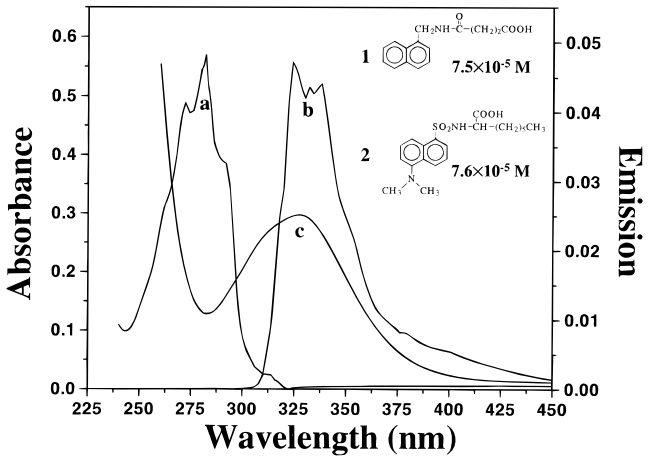

Figure 1. Absorbance (a) and normalized emission (b) spectra of naphthyl model compound **1** and absorbance spectrum (c) of dansyl model compound **2** in pH 8.0 aqueous buffer solution.

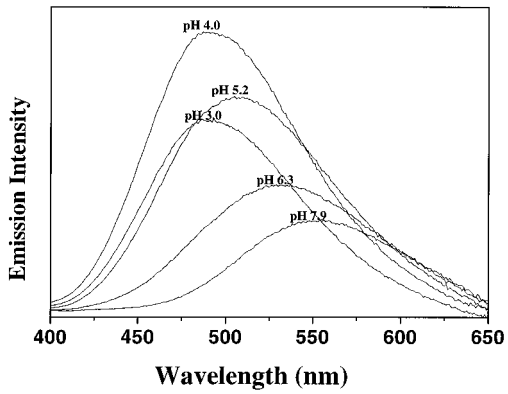

Figure 2. Emission spectra of the dansyl chromophore as a function of pH for singly-labeled copolymer (C8/C8-D8) at a concentration of 0.50 g/L in aqueous solution, when excited at 330 nm.

Steady-state fluorescence techniques were employed to examine the pH dependence of the association behavior for 30% *n*-octylamide hydrophobically modified poly(SM−EVE) in both aqueous solution and 6 M urea solutions, and unmodified poly(SM−EVE) also in aqueous solution. Figure 1 shows typical absorbance spectra for naphthyl and dansyl model compounds **1** and **2** in pH 8.0 aqueous buffer solutions. A maximum in the absorbance of the naphthalene species at 282 nm coincides with the absorbance minimum for the dansyl model compound. The dansyl model compound has an absorbance maximum at 330 nm, whereas the naphthalene species shows negligible absorbance at this wavelength and an overlap emission with absorbance of the dansyl chromophore. Thus, 282 nm was chosen as the excitation wavelength for studying naphthalene emission and 330 nm was chosen as the excitation wavelength for the dansyl emission.

Emission spectra were determined for the singly-labeled dansyl chromophores excited at 330 nm when attached to 30% *n*-octylamide-modified poly(SM−EVE) (C8/C8-D2 and C8/C8-D8) in aqueous solution and in 6 M urea, and when attached to unmodified poly(SM−EVE) (C0/C0-D2 and C0/C0-D8) in aqueous solution at a total polymer concentration of 0.5 g/L. Figure 2 shows typical emission spectra for the long-spaced dansyl label (C8/C8-D8) in aqueous solution at different pH values. The dansyl chromophore is a very sensitive probe and provides information about its microenvironment.[51,57,64−67]

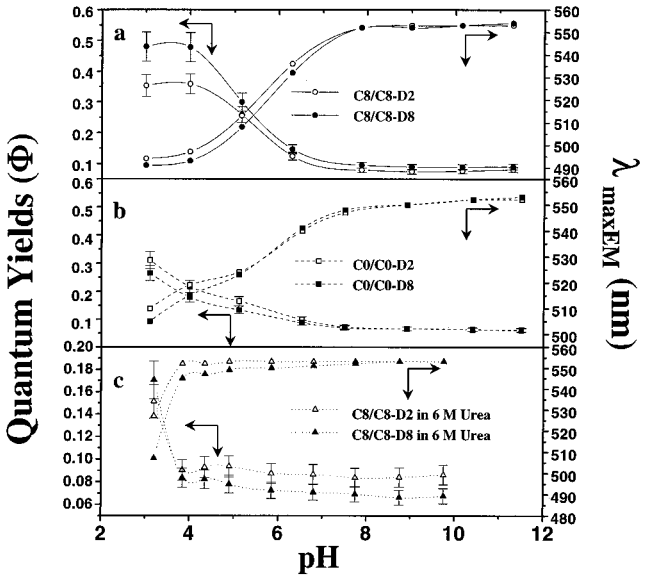

Figure 3. Plots of the fluorescence quantum yield and maximum emission wavelength as functions of pH for dansyl-labeled copolymers at a concentration of 0.50 g/L in aqueous solution.

This chromophore exhibits an enhancement in the fluorescence quantum yield and a blue shift of the emission peak as the microenvironment around the chromophore becomes more nonpolar. This behavior has been interpreted in terms of the polarity-dependent, twisted intramolecular charge-transfer (TICT) concept.[65−69]

Figure 3 shows the quantum yields and the wavelength at which maximum fluorescence emission occurs for dansyl-labeled polymers excited at 330 nm as a function of pH values. From Figure 3 (a) the maximum emission wavelength curve for dansyl labels on modified copoly(SM−EVE) in aqueous media is S-shaped in nature with the initial baseline deviation occurring at 495 nm, just below pH 4.0 for the short-spaced dansyl label and at 492 nm for the long-spaced dansyl label. The wavelength maximum reached is 555 nm at pH 7.0 for both labels. However, as shown in Figure 3b, the emission maximum for the dansyl labels on unmodified poly(SM−EVE) in aqueous solution exhibits a gradual red shift from 510 nm at pH 3.0 for the short-spaced labels and 505 nm for long-spaced labels to 550 nm at pH 7.0 for both. In Figure 3c, the emission maxima for the dansyl labels on hydrophobically modified poly(SM−EVE) in 6 M urea remain constant at 550 nm for both long- and short-spaced dansyl labels. Changes in quantum yields as a function of pH, shown in Figure 3a−c, mirror the changes indicated for the emission maxima, as anticipated.

In a study by Strauss and Vesnaver[55] on the free dansyl probe, it was found that the dansyl emission was characterized by two individual bands with maxima at 336 and 580 nm that correspond to emission from the excited states of the protonated and unprotonated forms of the dansyl probe, respectively, when excited at 268 nm, an isosbestic point. While the emission intensity at 336 nm was found to decrease with increasing pH, the emission intensity at 580 nm changed very little with pH. This was attributed to a large shift in the acid−base equilibrium of the dansyl group toward the unprotonated form as a result of excitation. However, in the case of an aqueous solution of dansyl-labeled poly(methacrylic acid),[66] the maximum emission wavelength of the dansyl label showed a gradual red shift from 495 to 562 nm with increasing pH when excited at 340 nm. Also, the emission intensity rose by a factor of 4.5 to a maximum at pH 4.2 and dropped dramatically by a factor of 18 upon changing to pH 6.9. Previous work[55,65−67] has shown that the maximum emission wavelength is affected negligibly by the ionization of the dansyl chromophore since only the unprotonated form is excited at 330 nm. In our work we have utilized fluorescence quantum yields rather than absolute intensities in order to account for the equilibrium shifts between protonated and unprotonated forms of the dansyl chromophore with changing pH. Thus, the changes in the fluorescence quantum yield and maximum emission wavelength of the dansyl chromophore should reflect the changing conformation of the polymer. It should be noted, however, that the experimental error is higher at low pH values since the number of "reporting" chromophores is quite small.

Above pH 7.0, the anionic carboxyl groups along the polymer backbone expand the coil by charge−charge repulsion, aiding the dissolution of the polymer in aqueous media. As a result, both the long- and short-spaced labels are forced into contact with water, resulting in a gradual increase of the maximum emission wavelength from 495 nm at pH 4.0 to 550 nm at pH 7.0 and a concomitant decrease of the fluorescence quantum yields (Figure 3a). Below pH 4.0, the polymer is more compact due to poorer hydration of carboxylic acid moieties (compared to carboxylate), hydrophobic interaction of the octyl groups, and hydrogen bonding. Differences in the dansyl label's ability to reside in a hydrophobic domain are especially evident with the fluorescence quantum yield for D8 being greater than that for D2.

Figure 3b, of unmodified poly(SM−EVE) in aqueous solution, illustrates fluorescence emission behavior typical of a well-solvated polyelectrolyte. Previous work[54,55] has shown that copoly(sodium maleate-*alt*-alkyl vinyl ether) has two acid−base equilibrium constants, $pK_{a1} = 3.8$ and $pK_{a2} = 6.6$. Above pK_{a2} the polymer is highly charged and exists in an extended conformation. This is indicated by the red-shifted maximum emission and the low quantum yields. As the pH is decreased and the carboxylate groups become protonated, a decrease in the extension is observed. In the modified polymer, this change is quite dramatic, as compared to that observed for the unmodified polymer.

Urea and its derivatives, which are well-known denaturants of proteins, are very efficient as modifiers of aqueous solution properties.[70,71] The addition of urea has been found to increase the critical micelle concentration (cmc) of ionic and nonionic surfactants due to an increase in the solubility of the hydrocarbon tails of the surfactants and a decrease in the aggregation number. In our case, the addition of urea to 0.5 g/L of 30% *n*-octylamide-modified poly(SM−EVE) directly disrupts hydrophobic association in the C8-substituted polymers. Lower quantum yields are observed and emission maxima are shifted to higher wavelengths for both D2 and D8 dansyl labels above pH 3.0. At lower pH, hydrogen bonding among the carboxylic acid groups combined with hydrophobic interactions, even in urea, are sufficiently strong enough to exclude water from the compact structures.

Nonradiative Energy Transfer (NRET) Studies. NRET studies utilizing the naphthyl donor (N1 or N8) and dansyl acceptor (D2 or D8) chromophores were

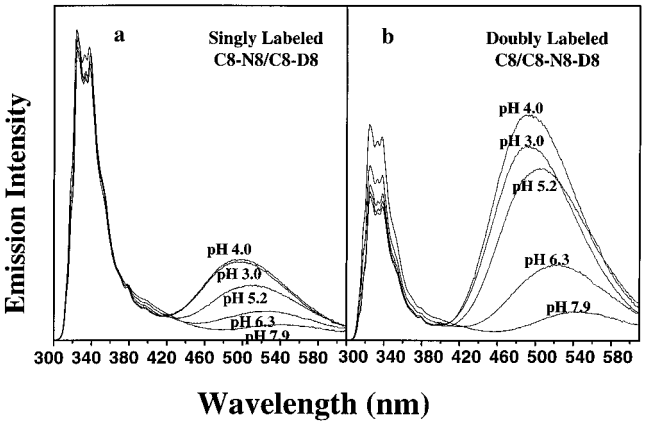

Figure 4. Change in the emission spectra vs pH for the long-spaced, labeled copolymer at a concentration of 0.50 g/L in aqueous solution, when excited at 282 nm.

conducted, and data were analyzed as described in the Experimental Section. The Förster distance for energy transfer for the naphthyl/dansyl donor/acceptor pair has been determined to be 23.45 Å.[60] Table 2 gives compositions of the solutions used in NRET studies utilizing simple designations. (C8/N1-D2-C8) designates an equimolar mixture of the unlabeled octylamide polymer with the doubly-labeled octyl-substituted polymer in which N1 represents the short naphthyl label and D2 the short dansyl label. (C8-N8/C8-D8) designates an equimolar mixture of octyl-substituted copolymers with long naphthyl and dansyl spacers.

Careful examination of these Ex-Em maps for solutions containing mixtures of singly-labeled and doubly-labeled polymers at high and low pH values (data not shown here) and consideration of Figure 1 reveal the utility of the label systems chosen during experimental design. Excitation at 282 nm, the maximum absorbance for the naphthyl group and the minimum for the dansyl chromophore, allows measurement of the fluorescence emission of the latter in the 450−580 nm range arising almost exclusively from NRET. Donor−acceptor positioning outside the Förster distance would result in weaker emission from the dansyl chromophore. However, simple tuning of the excitation wavelength to 330 nm (maximum absorbance of the dansyl label) leads only to fluorescence emission from the dansyl chromophore. This versatility is of considerable value in measuring distances via NRET as well as sampling the microenvironment of the labels with specific changes in pH, salt, temp, concentration, solvent character, etc.

Figure 4 shows emission intensity vs wavelength relationships for singly-labeled C8-N8/C8-D8 and doubly-labeled C8/C8-N8-D8 when excited at 282 nm. These two-dimensional "slices" of the more complete Ex-Em maps are quite instructive. In dilute solution at pH values above 7.0, little emission is observed in the 450−580 nm region for singly- or doubly-labeled systems. In the former case, since donors and acceptors are on separate chains, no mixing is expected in dilute solution (0.5 g/L). In the doubly-labeled system, intrachain repulsions at the low level of labeling are sufficient at pHs above 7.0−8.0 to allow chain expansion and to limit NRET. As the pH decreases, the doubly-labeled polymers (Figure 4b) show greatly enhanced emission intensity in the 430−580 nm range, indicating significant NRET. Simple coil contraction due to hydrogen-bonding between carboxylic acid groups, reduction of the "hydration shell", and hydrophobic association are consistent with increased NRET and Scheme 2. However, the behavior of the singly-labeled systems (Figure 4a), namely the increase of the emission intensity in the 430−580 nm range at low pH due to the hydrophobic effect, was not anticipated.

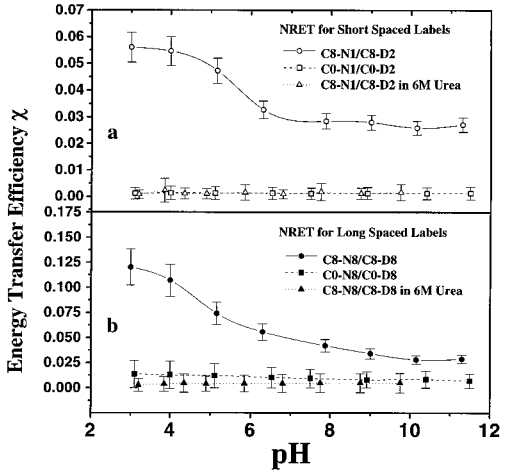

Figure 5. Plot of NRET quantum efficiency for mixtures of singly-labeled copolymers as a function of pH at a concentration of 0.50 g/L for (a) short-spaced labels and (b) long-spaced labels.

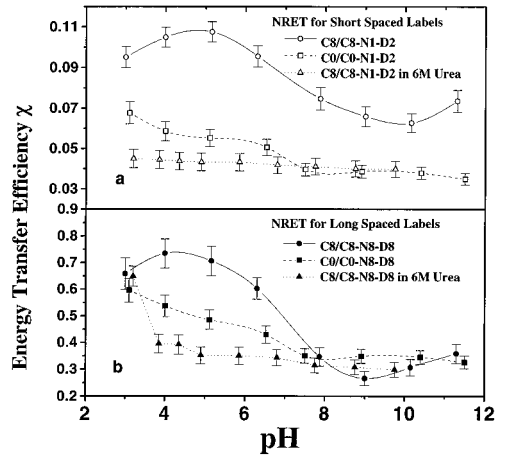

Figure 6. Plot of NRET quantum efficiency for mixtures of doubly-labeled copolymers as a function of pH at a concentration of 0.50 g/L for (a) short-spaced labels and (b) long-spaced labels.

We first considered the possibility of a small, but experimentally significant, contribution to emission intensity from direct excitation of the dansyl label at 282 nm. Utilizing the intensity data from Figure 4 and the modified Guillet equation (eq 2 in the Experimental Section), NRET quantum efficiencies were determined and corrected for direct excitation. Figures 5 and 6 present the resulting NRET quantum efficiency data as a function of pH.

In the experiments (Figure 5) in which separate dansyl-labeled and naphthyl-labeled chains were mixed, energy transfer efficiency was nearly zero across the full pH range for the controls (C0-N1/C0-D2) and (C0-N8/C0-D8) and for the octyl-substituted derivatives in 6 M urea. Somewhat surprising, however, are the small, but discernible, energy transfer efficiencies of approximately 0.03 above pH 8.0 for equimolar mixtures of the *n*-octylamide poly(SM−EVEs) independently labeled with dansyl and naphthyl groups. NRET increases 2-fold for C8-N1/C8-D2 and 3−4-fold for C8-N8/C8-D8 on decreasing pH to 4.0. Clearly, some intermolecular associations are occurring even at low concentrations, making neces-

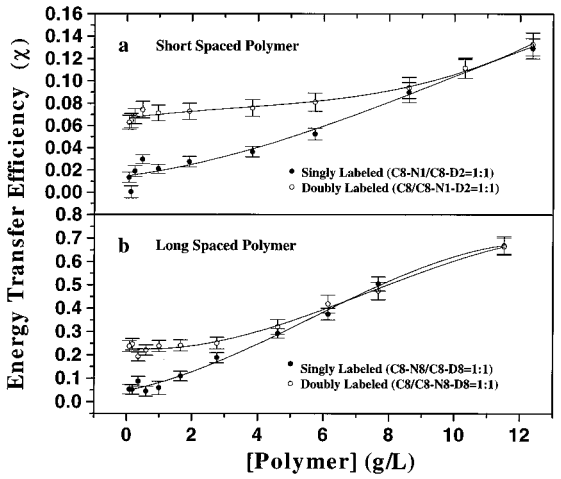

Figure 7. Plots of NRET quantum efficiency of hydrophobically modified copoly(SM−EVEs) as a function of the copolymer concentration in aqueous solution at pH 9.0 for (a) short- and (b) long-spaced labels.

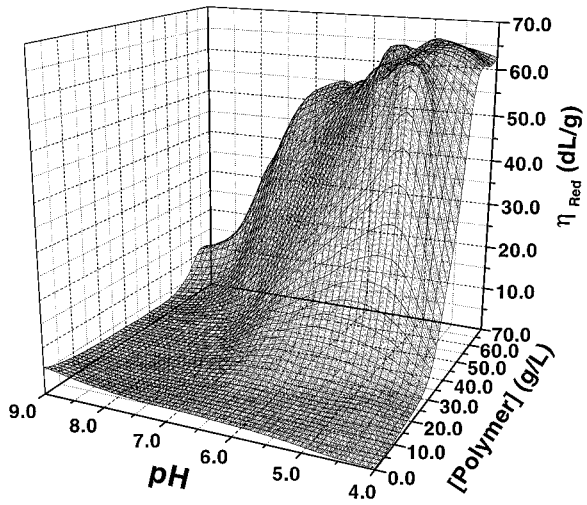

Figure 8. 3-D plot of reduced viscosity of hydrophobically modified copoly(SM−EVEs) as a function of pH and copolymer concentration in aqueous solution at a constant shear rate of 5.96 s^{-1} at 25 °C.

sary a reconsideration of the simple model depicted in Scheme 2a.

Figure 6 presents energy transfer efficiency data for the doubly-labeled systems. The S-shaped curves are consistent with globule-to-extended chain conformational change with increasing pH. The NRET efficiency for the C8/N1-D2-C8 polymer is approximately twice as high as that of the unmodified C0/N1-D2-C0 polymer across the entire pH range. For long spacers, all doubly-labeled systems exhibit similar NRET efficiencies above pH 7.0. Urea disrupts interaction across the entire range, yielding the lowest values of energy transfer.

In the absence of hydrophobic interactions along the polymer backbone, either induced by urea addition or inherent due to the lack of octyl substitution, the lower limit of energy transfer efficiency can be established for energy transfer along the chain. This is due to proximity of the donor/acceptor pairs along the hydrated chain. Over this pH range, longer spacer length samples exhibit energy transfer efficiency 6 times greater than those with short spacers. This is clearly associated with increased decoupling of the chromophore from the backbone. Enhanced energy transfer for both spacer lengths is observed at low pH, consistent with coil collapse and multiple chain association. The degree of NRET, however, is greatly enhanced for the octyl-modified doubly-labeled systems as compared to the controls as pH decreases.

Having extensively discussed the properties of the *n*-octyl-substituted poly(SM−EVEs) in the concentration regime dominated by intramolecular associations, we turn to NRET studies as a function of polymer concentration. Figure 7 follows NRET efficiency for singly- and doubly-labeled octyl-substituted polymers at pH 9.0 as the concentration is increased from 0.25 to 12.0 g/L. The NRET efficiency curves for the singly- and doubly-labeled polymers overlap at a concentration of 11 g/L for those with short-spaced labels and 7 g/L for those with long-spaced labels. With increasing concentrations of polymer, the distance between donors and acceptors decreases, resulting in enhancement of NRET for all species. The statistical positioning of donors and acceptors for the singly- and doubly-labeled polymers is equivalent at the intersection of the curves in Figure 7a,b. We interpret this as a microscopic indication of the critical overlap concentration, C^*, in the crossover from the dilute to semidilute concentration range.

Interesting comparisons can be made to rheological behavior by examining the reduced viscosity vs concentration plot of 30% C8-modified poly(SM−EVE). This plot shown in Figure 8 adds a third dimension—that of pH. The rheological value of C^*, as indicated by an upswing in the reduced viscosity, occurs at different points depending on pH. The onset changes from about 20 g/L at pH 4.0 to 60 g/L at pH 9.0. At intermediate pH values, the changes of slope of the viscosity−concentration curves are quite dramatic. The C^* value of 60 g/L at pH 9.0 is not quite 1 order of magnitude above that shown by NRET. We previously reported similar trends for high molecular weight, lightly substituted pyrenylsulfonamide copolymers of acrylamide which form concentration dependent intermolecular associations. The onset of association as measured by increases in excimer-to-monomer fluorescence intensities occurred approximately 1 order of magnitude below that observed by rheometry.[48,50] Also worth noting is the fact that the longer spacers apparently allow detection of association at lower concentrations. Since their motions are decoupled from that of the backbone, greater access to phase-separated microdomains is conformationally allowed.

Domain Size and Aggregation Number. In order to further interpret photophysical studies reported thus far, we carried out quasielastic light scattering (QELS) and aggregation number studies utilizing methods reported in literature for polymers forming associative domains. Concentrations were maintained at the same value of 0.5 g/L in both studies. Hydrodynamic diameters (d_H) were determined using quasielastic light scattering from the limiting coefficients, D_0, using the Stokes−Einstein equation:

$$D_0 = \frac{kT}{3\pi\eta_0 d_H} \tag{5}$$

where k is the Boltzmann constant, t is the absolute temperature, and η_0 is the viscosity of the solvent. Values of d_H appear in Table 3 and Figure 11 as a function of pH value. In Table 3, the hydrodynamic diameter (d_H) of 30% octyl hydrophobically modified copoly(SM−EVEs) in aqueous media is larger than that in 75 mM NaCl aqueous media over the same pH range due to the electrolyte shielding interactions in the latter.

Table 3. Hydrodynamic Diameters (d_H) for *n*-Octylamide-Modified Copoly(SM−EVEs) Measured by Dynamic Light Scattering[a]

			In Aqueous Media			
pH	3.1	4.6	5.8	7.2	8.8	10.2
d_H (nm)	77 ± 3	173 ± 9	275 ± 3	301 ± 7	273 ± 19	225 ± 4
			In 75 mM NaCl Aqueous Media			
pH	2.7	4.3	5.5	6.3	8.0	11.8
d_H (nm)	24 ± 3	32 ± 5	45 ± 5	49 ± 8	46 ± 8	41 ± 2

[a] Measured at 90 °C with 633 nm laser beam.

Table 4. Fluorescence Decay Parameters and N_{SSFQ} for 0.50 g/L of *n*-Octylamide-Modified Copoly(SM−EVEs) with and without 1.0 mM of 9-MA in Aqueous Solution

		naphthyl			9-MA			
system	pH	τ_1 (ns)/A_1	τ_2 (ns)/A_2	$\langle\tau\rangle$ (ns)	τ_1 (ns)/A_1	τ_2 (ns)/A_2	$\langle\tau\rangle$ (ns)	N_{SSFQ}
C8N8	2.9	30.8/91.83	6.12/8.17	30.4				
C8N8/9-MA	2.9	29.4/88.65	6.06/11.35	28.8	20.1/73.76	2.75/26.24	19.3	265 ± 17
C8N8	8.9	25.7/89.12	8.34/10.88	25.0				
C8N8/9-MA	8.9	25.1/85.31	12.3/14.39	24.1	18.2/57.42	4.75/42.58	16.0	4 ± 3
C8N2	1.8	29.7/90.20	6.05/9.80	29.2				
C8N2/9-MA	1.8	29.2/91.30	5.96/8.70	28.8	18.0/8.25	6.25/91.75	8.67	220 ± 15
C8N2	9.1	28.3/89.38	6.57/10.62	27.7				
C8N2/9-MA	9.1	27.5/87.58	5.57/12.42	27.5		6.13/100	6.13	7.5 ± 4
C8/Naph	2.2	29.1/85.34	6.00/14.66	28.3				
C8/Naph/9-MA	2.2	28.7/83.30	5.86/16.70	27.8	17.3/10.35	6.65/89.65	9.11	120 ± 12
C8/Naph	9.1	26.3/80.28	6.77/19.72	25.1				
C8/Naph/9-MA	9.1	25.7/79.56	5.87/20.44	24.6	15.53/8.75	5.32/91.25	7.55	8 ± 3

As the pH value increases to 7.0, the respective hydrodynamic diameters (d_H) of the copoly(SM−EVEs) in aqueous media and in 75 mM NaCl increase. This is consistent with a gradual change from a compact globule to a more solvated coil. Above pH 7.0, however, the hydrodynamic diameters decrease due to increased ionic strength. As would be expected, collapse is not as dramatic for the solutions already containing 75 mM NaCl.

The relative size of the polymeric micelles was determined using fluorescence quenching of the naphthyl chromophore by 9-methylanthracene (9-MA) as a function of pH. Such luminescence quenching techniques have been previously reported for investigations of the aggregation number of surfactants[71] and "polysoaps."[36,37] The basic premise underlying this technique is that in an aqueous solution, the chromophore and quencher are partitioned into micellar domains. Poisson statistical quenching kinetics can then be used to estimate the mean aggregation number of the polymeric micelles.

Most aggregation number studies have utilized probe molecules, for example, the tris(2,2′-bipyridine)ruthenium(II) ion [$Ru(bpy)_3^{2+}$] and 9-methylanthracene, which undergo Perrin-type quenching. Here we utilize naphthalene/9-methylanthracene which transfers energy by a Förster-type mechanism. This pair is quite useful in our studies since (a) we avoid direct binding of ionic sites with chromophore and (b) naphthalene can be studied easily as a probe or label in the C8-modified poly(SM−EVEs). The Förster distance for this pair (24 Å)[31,43] is quite small compared to domain size. Aggregation numbers determined by this method will, of course, depend on proximity rather than contact of the energy transfer pairs.

Depending on the donor/quencher pair, either steady-state or dynamic quenching experiments may be performed to determine aggregation numbers. The applicability of either technique must first be evaluated. In order to confirm the predominance of the static quenching process in this study, time-resolved fluorescence measurements were performed at a concentration of 21.0 μM of naphthyl chromophore in the presence and absence of 1.0 mM of 9-MA at selected high and low pH values. The decay curves of the naphthyl chromophore and 9-MA were monitored at 325 and 415 nm, respectively, with an excitation wavelength of 282 nm. Fluorescence decay data were analyzed using software obtained from Edinburgh Instruments. The average fluorescence lifetime was calculated using the relationship $\langle\tau\rangle = \sum A_i\tau_i^2/\sum A_i\tau_1$, in which A_i is the pre-exponential factor and τ_i is the fluorescence lifetime. The parameters of fluorescence decay at various pH values along with aggregation numbers obtained by SSFQ are shown in Table 4.

The average fluorescence lifetimes of naphthyl chromophores at the high pH value (∼9.0) are ∼2−5 ns shorter than those at the low pH value (∼2.0) in both the presence and absence of 9-MA. The small change in lifetime is attributed to pH-induced microenvironmental changes around the naphthyl chromophore.[56] This effect was previously demonstrated with the dansyl-labeled samples (Figure 2). In addition, the average fluorescence lifetime of the naphthyl chromophores in the presence of 1.0 mM 9-MA at the same pH is just slightly less (5%) than that in the absence of 9-MA. This indicates that static quenching is the dominant quenching process and affirms the applicability of steady-state fluorescence methods for the determination of aggregation numbers.

For the steady-state fluorescence quenching (SSFQ) aggregation number study, the emission spectra of naphthyl chromophores as sequestered probes or as covalent moieties attached by short (N1) or long (N8) spacers were measured in the presence of increasing amounts of a quencher, 9-MA. Figure 9 shows typical changes in the emission spectra at pH 4.3 for the 30% hydrophobically modified C8-N8 at a concentration of 0.50 g/L (21.0 μM of naphthyl chromophore). Fluorescence intensity data gathered from similar studies at specified pH values were then plotted as a function of 9-MA concentration (Figure 10). Using eqs 3 and 4, the aggregation numbers (NSSFQ) at each pH value were determined. These aggregation number values are

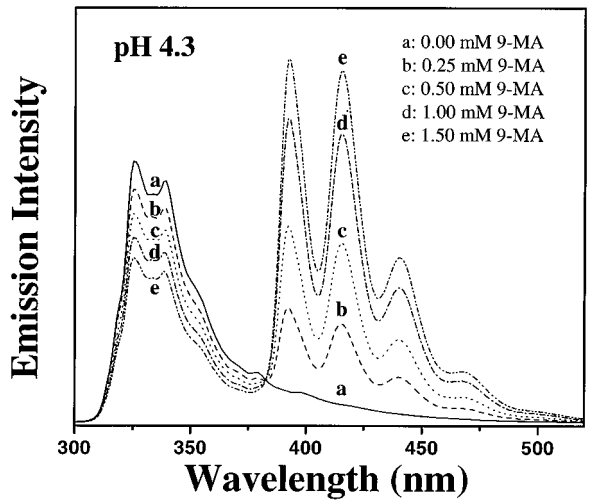

Figure 9. Change in the emission intensity vs concentraion of 9-MA for long-spaced naphthyl-labeled C8-N8 at a concentration of 0.50 g/L (21.0 μM of naphthyl chromophore) in aqueous solution with a pH value of 4.3, when excited at 282 nm.

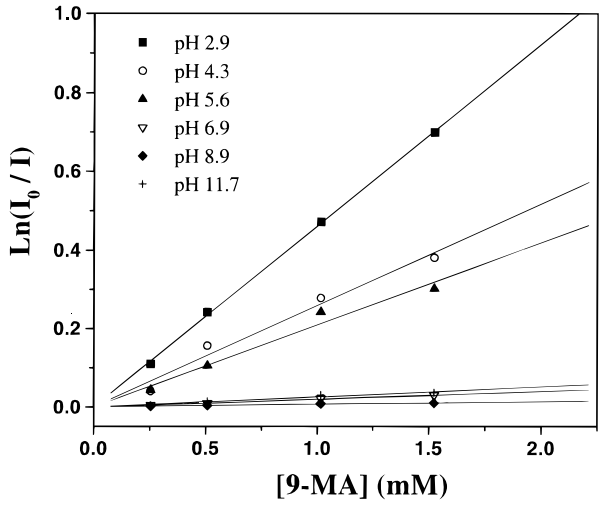

Figure 10. Plot of $\ln(I_0/I)$ vs 9-MA concentration for C8-N8 (0.50 g/L aqueous solution) excited at 282 nm at various pH values.

shown as a function of pH in Figure 11, along with the hydrodynamic radii (Table 3) obtained from dynamic light scattering.

Perhaps the most significant information to be gleaned from Figure 11 is the variation of NSSFQ with changing pH. Aggregation numbers measured by probe/quencher techniques are almost universally accepted for surfactant-like micelles. However, the exact meaning when applied to hydrophobically associating macromolecular entities has been debated. Some authors have suggested single domains[72] for "polysoap" systems, while others have proposed multiple domains[36−39] along a single chain. Here we simply assume NSSFQ represents the number of hydrophobes involved in microdomain formation as measured by the proximity of our naphthalene/9-MA pair within the Förster distance of 24 Å.[31,43] For the 30% C8-modified poly(SM−EVEs) of molecular weight 3.5×10^5, approximately 400 octyl units are present on each chain. In our opinion aggregation numbers can be used in a qualitative manner only to describe liaisons of hydrophobic entities at a given environmental condition.

In Figure 11 aggregation numbers and hydrodynamic diameter values from dynamic light scattering (Table

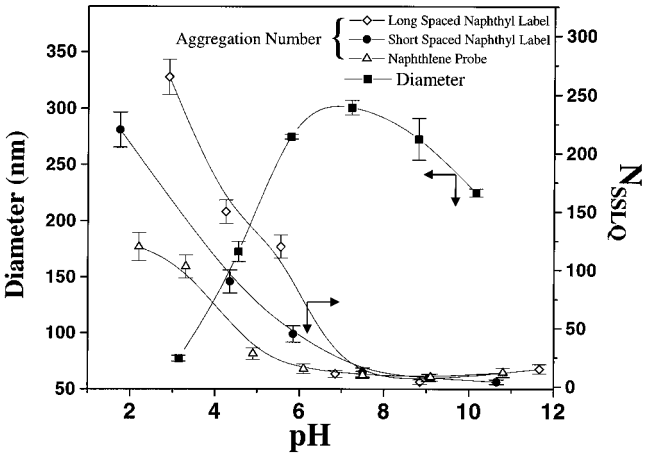

Figure 11. Plot of the hydrodynamic diameter determined by dynamic light scattering and aggregation number measured by steady-state fluorescence quenching as a function of pH in aqueous solution at a concentration of 0.50 g/L for 30% octylamide-modified poly(SM−EVEs).

3) are shown as a function of pH. As the pH values increase to pH ~6.7, the aggregation numbers decrease, which is consistent with a polysoap-to-polyelectrolyte (globule-to-extended chain) transition. The drop in value with decreasing pH must also be considered in terms of the NRET results on singly-labeled polymers. Since our studies on mixtures of singly-labeled chains in dilute solutions show the lowest NRET above pH 6.7, it would seem likely that multiple associations along the chain are present. The 30% hydrophobically modified copoly(SM−EVEs) having longer spaced naphthyl labels show the largest values of NSSFQ due to the decoupling effects of the long spacer from the polymer backbone facilitating partitioning into hydrophobic domains. Since the probe would represent a chromophore completely decoupled from the polymer backbone, it would logically follow that the system with the naphthalene probe should exhibit the highest amount of quenching and the largest aggregation numbers. This, however, is not the case. One simple explanation is based on greater solubility of the naphthalene probe in water compared to its solubility as attached to the spacers. This small but significant effect would result in the smallest aggregation numbers (NSSFQs) due to the distribution the chromophore between the solution phase and the hydrophobic microheterogeneous domains. Although the naphthyl probe and labels each provide different apparent aggregation numbers as a function of pH, the trends for each chromophore are the same and are consistent with a polysoap-to-polyelectrolyte transition, as discussed above.

Conclusions

The series of naphthyl- and/or dansyl-labeled, *n*-octyl-substituted poly(SM−EVEs) synthesized for this study has allowed examination of microdomain ordering in aqueous media. By utilizing a combination of techniques including viscometry, dynamic light scattering, and fluorescence quenching, we can more fully elucidate the nature of hydrophobic association as a function of pH and polymer concentration. Several features of the classical conceptual model shown in Scheme 2 are consistent with our studies. At low polymer concentrations (0.5 g/L), the 30% *n*-octyl-substituted copolymers undergo a hypercoil or globule-to-extended chain conformational change with increasing pH. This transition is similar to that reported by Strauss and later by other

groups for hydrolyzed n-alkyl vinyl ether/maleic anhydride copolymers. The globule-to-extended chain transition, sometimes called the "polysoap-to-polyelectrolyte" transition, is accurately followed by observing the fluorescence quantum yields and maximum emission wavelengths of dansyl-labeled polymers, as well as NRET on doubly-labeled (dansyl-naphthyl) or mixtures of the individual polymers with these donors or acceptors. This transition is not seen when domains are disrupted by addition of 6 M urea or in the unmodified controls.

The hydrolyzed structure of *n*-octyl poly(SM−EVE) possesses two carboxyl moieties with pK_a values reported to be 3.8 and 6.6, respectively. As the pH is raised progressively beyond 6.7, disruption of hydrophobic clusters occurs with the aggregation number greatly reduced. In other words, fewer of the 400 octyl groups along a singular chain are involved in any type of microdomain with increasing pH. Only a small number of encounters occur between singly-labeled donor and singly-labeled acceptor chains; therefore, the NRET quantum efficiency is at its lowest point. The same is true for the doubly-labeled (both naphthyl and dansyl groups) chains. However, even at high pH some labels (as shown by the controls) are close enough along the same chain for some NRET. A maximum in hydrodynamic volume as measured by light scattering and viscosity occurs in the pH 7−8 range. The quantum yield for the fluorescence of the dansyl-labeled chains is at a minimum while the λ_{max} is at a maximum. The slight decrease in hydrodynamic volume as observed by light scattering and viscometry with added NaOH at high pH is due to increased ionic strength.

As pH is lowered below pK_{a1} and pK_{a2}, ionization is insufficient to disrupt hypercoiling caused by the large number of octyl groups along the chain. At intermediate pH values in the transition region, a solvated corona around a less hydrated core is envisioned. The core becomes more collapsed with a continued decrease in pH. Hydrogen-bonding between the carboxylic acid groups excludes water. The environment reported by the dansyl labels (at least those unprotonated) is much more constricted and less hydrated. NRET is at its highest level for the doubly-labeled polymer, as expected. Surprisingly, NRET is also observed for the mixed singly-labeled polymer, suggesting multichain aggregation at low pH. It seems unlikely that statistical collisions would take place within the Förster distance as the individual chains collapse in dilute solution, especially since the labels are covalently attached. We conclude, therefore, that the simple model in Scheme 2 should be modified to show unimer/multimer equilibria much like those often reported for protein associations. The dynamics of this type of association in polysoaps remain unclear.

Association also occurs with increasing polymer concentration. Intermolecular domain association appears near a concentration of 60 g/L at pH 9.0, as measured by rotational viscometry. However, this onset is seen on a molecular level much earlier by NRET, near 7 g/L for the long spacer mixtures (N8-D8) and 11 g/L for the N1-D2 containing polymers. The value of C^* changes dramatically with pH.

The remarkable effects of alkyl substitution on microphase separation and the potential of reversible domain formation in amphiphilic polymers present a number of opportunities as well as challenges in tailoring responsive aqueous polymers with sequestration and viscosification properties. Experimental data of the type reported here need to be coupled with emerging theoretical treatments in order to direct future synthetic efforts toward commercial systems with ultimate utility.

Acknowledgment. The U.S. Department of Energy, the U.S. Office of Naval Research, the Gillette Corp., ICI, and Nalco are gratefully acknowledged for their support of our research efforts.

References and Notes

(1) *Water-Soluble Polymers*; Bikales, N. M., Ed.; Plenum Press: New York, 1973.
(2) *Encyclopedia of Polymer Science and Engineering*, 2nd ed.; McCormick, C. L., Bock, J., Schulz, D. N., Eds.; John Wiley & Sons, Inc.: New York, 1989; Vol. 17.
(3) *Water-Soluble Synthetic Polymers: Properties and Behavior*; Molyneaux, P., Ed.; CRC Press: Boca Raton, FL, 1984.
(4) *Water-Soluble Polymers: Synthesis, Solution Properties, and Applications*; Shalaby, S. W., McCormick, C. L., Butler, G. B., Eds.; ACS Symposium Series No. 467; American Chemical Society: Washington, DC, 1991.
(5) Morgan, S. E.; McCormick, C. L. *Prog. Polym. Sci.* **1990**, *15*, 507.
(6) Tsiourvas, D.; Paleos, C. M.; Dais, P. *J. Appl. Polym. Sci.* **1989**, *38*, 257.
(7) Tsiourvas, D.; Paleos, C. M. *J. Polym. Sci., Polym. Chem. Ed.* **1990**, *28*, 1263.
(8) *Polymer as Rheology Modifiers*; Schulz, D. N., Glass, J. E., Eds.; ACS Symposium Series No. 462; American Chemical Society: Washington, DC, 1991.
(9) McCormick, C. L.; Chang, Y. *Macromolecules* **1994**, *27*, 2151.
(10) Branham, K. D.; Davis, D. L.; Middleton, J. C.; McCormick, C. L. *Polymer* **1994**, *35*, 4429.
(11) Zhang, Y.; Wu, C.; Fang, Q.; Zhang, Y-X. *Macromolecules* **1996**, *29*, 2494.
(12) Biggs, S.; Hill, A.; Candau, F. *J. Phys. Chem.* **1992**, *96*, 1505.
(13) Borochov, N.; Eisenberg, H. *Macromolecules* **1994**, *27*, 1440.
(14) Branham, K. D.; Snowden, H. S.; McCormick, C. L. *Macromolecules* **1996**, *29*, 254.
(15) Newman, J. K.; McCormick, C. L. *Macromolecules* **1994**, *27*, 5114.
(16) Uemura, Y.; Macdonald, P. M. *Macromolecules* **1996**, *29*, 63.
(17) Morishima, Y. *Prog. Polym. Sci.* **1990**, *15*, 949.
(18) Turro, N. J.; Gratzel, M.; Braun, M. *Angew. Chem., Int. Ed. Engl.* **1980**, *18*, 675.
(19) Webber, S. E. *Chem. Rev.* **1990**, *90*, 1469.
(20) Morawetz, H. *Science* **1988**, *240*, 172.
(21) Itoh, Y.; Satoh, H.; Yasue, T.; Hachimori, A.; Satozono, H.; Suzuki, S.; Webber, S. E. *Macromolecules* **1994**, *27*, 1434.
(22) Ringsdorf, H.; Simon, J.; Winnik, F. M. *Macromolecules* **1992**, *25*, 5353, 7306.
(23) Schild, H. G.; Tirrell, D. A. *Macromolecules* **1992**, *25*, 4553.
(24) Winnik, F. M. *Macromolecules* **1989**, *22*, 734.
(25) Arora, K. S.; Hwang, K.-C.; Turro, N. J. *Macromolecules* **1986**, *19*, 2806.
(26) Morishima, Y.; Ohgi, H.; Kamachi, M. *Macromolecules* **1993**, *26*, 4293.
(27) Bai, F.; Chang, C.-H.; Webber, S. E. *Macromolecules* **1986**, *19*, 2484.
(28) Duhamel, J.; Yekta, A.; Hu, Y. Z.; Winnik, M. A. *Macromolecules* **1992**, *25*, 7024.
(29) Zeng, W.; Shirota, Y. *Macromolecules* **1989**, *22*, 4204.
(30) Morishima, Y.; Lim, H. S.; Nozakura, S.; Sturtevant, J. L. *Macromolecules* **1989**, *22*, 1148.
(31) Bai, F.; Webber, S. E. *Macromolecules* **1988**, *21*, 628.
(32) Morishima, Y.; Kobayashi, T.; Nozakura, S.; Webber, S. E. *Macromolecules* **1987**, *20*, 807.
(33) Sturtevant, J. L.; Webber, S. E. *Macromolecules* **1989**, *22*, 3564.
(34) Cao, T.; Yin, W.; Webber, S. E. *Macromolecules* **1994**, *27*, 7459.
(35) Anthony, O.; Zana, R. *Macromolecules* **1994**, *27*, 3885.
(36) Zdanowicz, V.; Strauss, U. P. *Macromolecules* **1993**, *26*, 4770.
(37) Hsu, J.-L.; Strauss, U. P. *J. Phys. Chem.* **1987**, *91*, 6238.
(38) Chu, D.-Y.; Thomas, J. K. *Macromolecules* **1987**, *20*, 2133.
(39) Binana-Limbele, W.; Zana, R. *Macromolecules* **1990**, *23*, 2731.
(40) Hargreaves, J.; Webber, S. E. *Macromolecules* **1982**, *15*, 424.
(41) Itoh, Y.; Nakada, M.; Satoh, H.; Hachimori, A.; Webber, S. E. *Macromolecules* **1993**, *26*, 1941.
(42) Nagata, I.; Morawetz. H. *Macromolecules* **1981**, *14*, 87.

(43) Guillet, J. E.; Rendall, W. A. *Macromolecules* **1986**, *19*, 224.
(44) Pispisa, B.; Variano, M.; Palleschi, A.; Zanotti, G. *Macromolecules* **1994**, *27*, 7800.
(45) Major, M. D.; Torkelson, J. M.; Brearley, A. *Macromolecules* **1990**, *23*, 1700.
(46) Hu, Y.; Kramer, M. C.; Boudreaux, C. J.; McCormick, C. L. *Macromolecules* **1995**, *28*, 7100.
(47) Kramer, M. C.; Steger, J. R.; Hu, Y.; McCormick, C. L. *Macromolecules* **1996**, *29*, 1992.
(48) McCormick, C. L.; Hoyle, C. E.; Clark, M. D. *Macromolecules* **1990**, *24*, 3124; **1991**, 24, 2397.
(49) Ezzell, S. A.; McCormick C. L. *Macromolecules* **1992**, *25*, 1881.
(50) Ezzell, S. A.; Hoyle, C. E.; Creed, D.; McCormick C. L. *Macromolecules* **1992**, *25*, 1887.
(51) Strauss, U. P.; Schlesinger, M. S. *J. Phys. Chem*. **1978**, *82*, 1627.
(52) Dubin, P.; Strauss, U. P. *J. Phys. Chem*. **1970**, *74*, 2842.
(53) Martin, P. J.; Strauss, U. P. *Biophys. Chem*. **1980**, *11*, 397.
(54) Strauss, U. P.; Gershfeld, N. L. *J. Phys. Chem*. **1954**, *58*, 747.
(55) Strauss, U.; Vesnaver, G. *J. Phys. Chem*. **1975**, *79*, 1558, 2426.
(56) Hu, Y.; Armentrout, R. S.; McCormick, C. L. Submitted to *Macromolecules*.
(57) Shea, K. J.; Stoddard, G. J.; Shavelle, D. M.; Wakui, F.; Choate, R. M. *Macromolecules* **1990**, *23*, 4497.
(58) Rusakowicz, R.; Testa, A. C. *J. Phys. Chem*. **1968**, *72*, 2680.
(59) Eastmen, J. W. *Photochem. Photobiol.* **1967**, *6*, 55.
(60) Lakowicz, J. R.; Wiczk, W.; Gryczynski, I.; Fishman, M.; Johnson, M. *Macromolecules* **1993**, *26*, 349.
(61) Binana-Limbele, W.; Zana, R. *Macromolecules* **1987**, *20*, 1331.
(62) McCormick, C. L.; Nonaka, T.; Johnson, C. B. *Polymer* **1988**, *29*, 731.
(63) Morishima, Y.; Kobayashi, T.; Nozakura. S. *Polym. J*. **1989**, *21*, 267.
(64) Li, Y. H.; Chan, L. M.; Tyer, L.; Moody, R. T.; Himel, C. M.; Hercules, D. M. *J. Am. Chem. Soc.* **1975**, *97*, 3118.
(65) Bednar, B.; Morawetz, H.; Shafer, J. *Macromolecules* **1985**, *18*, 1940.
(66) Hu, Y.; Horie, K.; Ushiki, H. *Macromolecules* **1992**, *25*, 6040.
(67) Kosower, E. M.; Dodiuk, H.; Tanizawa, K.; Ottolenghi, M.; Orbach, N. *J. Am. Chem. Soc.* **1975**, *97*, 2167.
(68) Bhattacharyya, K.; Chowdhury, M. *Chem. Rev*. **1993**, *93*, 507.
(69) Ruiz, C. C. *Colloid Polym. Sci*. **1995**, *273*, 1033.
(70) Grieser, F.; Lay, M.; Thistlethwaite, P. J. *J. Phys. Chem*. **1985**, *89*, 2065.
(71) Turro, N. J.; Tekta, A. *J. Am. Chem. Soc.* **1978**, *100*, 5951.
(72) Chu, D-Y.; Thomas, J. K. *Macromolecules* **1991**, *24*, 2212.

MA9613502